

## A model for cytochrome oxidase

(magnetic circular dichroism/magnetic susceptibility/antiferromagnetic coupling/electron transfer)

GRAHAM PALMER\*, GERALD T. BABCOCK\*, AND LARRY E. VICKERY†

\* Department of Biochemistry, Rice University, Houston, Texas, 77005; and † Laboratory of Chemical Biodynamics, University of California, Berkeley, Calif. 94720

Communicated by David E. Green, April 2, 1976

**ABSTRACT** A model is proposed for the active center of cytochrome *c* oxidase (ferrocytochrome *c*:oxygen oxidoreductase, EC 1.9.3.1) in which cytochrome *a* is a low-spin ferrihemoprotein and cytochrome *a*<sub>3</sub> is a high-spin ferrihemoprotein antiferromagnetically coupled to one of the two Cu<sup>2+</sup> ions present in the enzyme. It is further proposed that reduction is accompanied by a conformational change in the enzyme thus exposing the sixth coordination site of cytochrome *a*<sub>3</sub> to ligands.

With this model it is possible to account for a variety of outstanding observations including the results of magnetic circular dichroism, Mossbauer, and electron paramagnetic resonance spectroscopies, as well as magnetic susceptibility measurements.

It is now well established that cytochrome oxidase (ferrocytochrome *c*: oxygen oxidoreductase, EC 1.9.3.1) contains equimolar amounts of heme *a* and copper, and it is most probable that the minimal functional unit contains two mole of heme and two of copper. Because four equivalents of reductant are required to fully reduce the oxidized enzyme (1), it is believed that the metal ions are oxidized, presumably Fe<sup>3+</sup> for the heme iron and Cu<sup>2+</sup> for the copper. With this composition, the enzyme is able to accommodate all four electrons from the reducing substrate before transferring them to oxygen in what is, effectively, a coordinated reaction at room temperature (2).

The electron paramagnetic resonance (EPR) spectrum of the enzyme exhibits an axially symmetric resonance (3) close to  $g = 2$  (similar to Type 1 copper proteins), and although the EPR assigned to Cu<sup>2+</sup> in cytochrome oxidase exhibits no hyperfine splitting at  $g_{\parallel}$ , the spectrum has been simulated (4) with a hyperfine splitting constant about one-sixth of the normal value. This large reduction in the hyperfine interaction has yet to be explained. The resonance disappears on addition of reductants, and the rate of both this process and its reappearance on oxidation of reduced protein is very rapid.

A second species identified by EPR is a low-spin heme present in the resting (oxidized) enzyme (5). Additional heme resonances, both high-spin and low-spin, are seen at intermediate states of reduction produced either statically or kinetically, and the relative amounts of these species are readily changed by the addition of heme ligands to the reaction mixture (5). There is, however, a major dilemma in that the intensity of both the Cu<sup>2+</sup> and Fe<sup>3+</sup> resonances observed in the resting enzyme only accounts for 0.8 mol of Cu<sup>2+</sup> and 1.0 mol of Fe<sup>3+</sup> per functional unit, though there is evidence that the intensity of the copper EPR is increased in certain reoxidation experiments (6).

A second puzzling property of resting cytochrome oxidase is its poor reactivity with reagents recognized as effective ferric heme ligands. For example, while the reaction of the oxidase

with sodium azide is rapid, the changes in the visible spectrum are extremely small (7) and make it quite unlikely that the reaction of the azide is with heme iron. This is in contrast to the ready reaction of partially reduced oxidase with azide which results in the conversion of a high-spin EPR signal to a low-spin one and demonstrates that the reaction is indeed with a heme iron under these conditions. Cyanide (8) and sulfide (9) behave similarly and it seems credible that the heme sites in the resting oxidase are blocked, but, upon reduction, a structural change occurs which exposes the liganding site to exogenous reagents. With very long incubation times, reaction of exogenous ligands with the small, steady-state concentration of conformationally perturbed molecules might occur.

The Soret region of the magnetic circular dichroism (MCD) (7) spectrum of ferricytochrome oxidase exhibits a derivative-shaped curve with a zero-crossing near 428 nm (Fig. 1), and the temperature dependence of the spectrum establishes that it is composed predominantly of Faraday *C* terms (10). It has been shown for other hemeprotein systems that the amplitude of this MCD band is a function of the amount of low-spin hemichrome present (11) and, by comparison of our data on cytochrome oxidase with that obtained on model heme *a* compounds, we estimate that approximately 50% of the heme *a* in the oxidase is in the low-spin state (10). We interpret this observation to mean that ferricytochrome oxidase contains one low-spin ( $S = \frac{1}{2}$ ) heme *a* and one high-spin ( $S = \frac{5}{2}$ ) heme *a*.

On reduction, the MCD in the Soret region changes sign and becomes more intense (Fig. 1); it also exhibits a temperature dependence indicating that it arises from a paramagnetic center (10). The shape of the MCD spectrum is very similar to that observed for high-spin deoxymyoglobin (11) and deoxyhemoglobin (12), but the intensity on a total heme *a* basis is approximately half that found for these proteins. Low-spin ferrous heme centers exhibit variable MCD intensity in the Soret region, but being diamagnetic their contributions can be resolved by low temperature experiments. We interpret these results to mean that ferrocytochrome oxidase possesses one low-spin ( $S = 0$ ) and one high-spin ( $S = 2$ ) heme *a*.

The simplest interpretation of these data is that both oxidized and reduced cytochrome oxidase contains one high-spin and low-spin heme and the heme that is high-spin in the oxidized cytochrome oxidase is also high-spin in the reduced enzyme.

But if one of the hemes is in the high-spin state when the enzyme is oxidized, it should be observable by EPR for ferrihemoproteins have characteristic and easily detectable EPR spectra (14); these have not been detected despite substantial efforts.

A sensible resolution of this difficulty resides in a suggestion by Van Gelder and Beinert (5), explored theoretically by J. S. Griffith (15), that both the invisible heme and invisible copper are present as an exchange-coupled complex of even spin ( $S = 2$  or 3) which would be difficult or impossible to observe by EPR. An alternative explanation requires that these species are

Abbreviations: EPR, electron paramagnetic resonance spectroscopy; MCD, magnetic circular dichroism spectroscopy; *S*, electron spin.

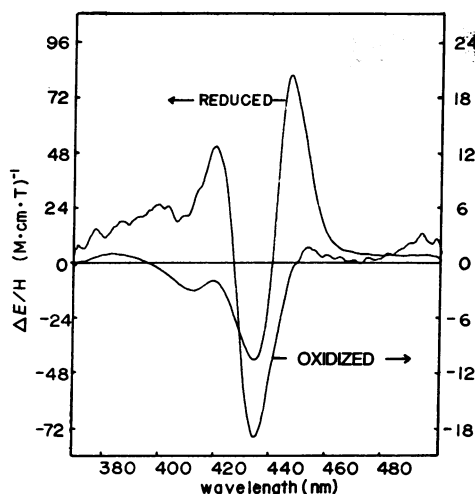


FIG. 1. Magnetic circular dichroism spectra of oxidized and reduced beef heart cytochrome oxidase. The enzyme was prepared by the method of Hartzell and Beinert (28), but similar results were obtained with enzyme prepared by three other published procedures, and on a sample of yeast cytochrome oxidase. The data are expressed on a per heme basis; spectra were recorded at 4° as previously described (13). *E*, extinction coefficient; *H*, magnet field; *T*, tesla = 10 kilogauss.

rendered undetectable by dipole-dipole broadening; however, the computed EPR spectrum of a low-spin heme-Cu<sup>2+</sup> pair shows intense features even at distances as short as 4 Å (G. Palmer, unpublished calculations).

We propose that the cytochrome oxidase unit comprises one low-spin ferrihemoprotein, one magnetically isolated Cu<sup>2+</sup>, and an antiferromagnetically spin-coupled dimer comprising a cupric ion and a high-spin ferrihemoprotein (Fig. 2).

We equate the low-spin ferrihemoprotein with cytochrome *a* and assign it the most positive value for a reduction potential (16). The nature of the axial ligands X and Y coordinating the iron are not determined but are of sufficient ligand field strength to favor the low-spin state. The EPR detectable Cu<sub>A</sub><sup>2+</sup> must have an unusual coordination geometry for not only are its *g*-values closer to two than for any other copper protein, but its hyperfine splitting constant is so small that the hyperfine pattern is totally unresolved. We do not assign specific ligands here either, but in view of the propensity of sulfur ligation to attenuate the hyperfine interaction (17) one might speculate

that two or more sulfur atoms are in the coordination sphere of this metal ion; alternatively, a single sulfur atom plus non-planar coordination geometry might be responsible for the unique EPR (18). Cu<sub>A</sub><sup>2+</sup> is assigned a potential more negative than cytochrome *a* (16).

The proposed structure of the antiferromagnetic complex between Cu<sub>B</sub><sup>2+</sup> and the high-spin heme component (hereafter called cytochrome *a*<sub>3</sub>) rides on several pieces of evidence. Blokzijl-Homan and Van Gelder (19) have demonstrated that NO binds to one of the two hemes of cytochrome oxidase which is presumably *a*<sub>3</sub> on the basis of the competition between NO and CO (20). This NO complex exhibits a 9 line hyperfine pattern at *g*<sub>z</sub> similar to many other hemoproteins (14, 21), and its presence is evidence for the presence of nitrogen as the ligating function *trans* to the nitric oxide, though the identity of the specific residue is not established by this observation. However, the proposed antiferromagnetic coupling with the adjacent Cu<sub>B</sub><sup>2+</sup> requires a bridging function between the two metal ions and this role is admirably filled by histidine (Fig. 2). This bridging ability for histidine has recently been demonstrated in the x-ray structure of the enzyme superoxide dismutase (EC 1.15.1.1) where an imidazole ring simultaneously coordinates both the cupric and zinc ions via its two nitrogen atoms (22). Metal substituted derivatives of superoxide dismutase of composition (Cu<sup>2+</sup>)<sub>4</sub> and (Cu<sup>2+</sup>)<sub>2</sub>(Co<sup>2+</sup>)<sub>2</sub> [compared to (Cu<sup>2+</sup>)<sub>2</sub>(Zn<sup>2+</sup>)<sub>2</sub> in the native protein] are magnetically abnormal with EPR and magnetic susceptibility properties (23) diagnostic of antiferromagnetic interactions. One thus infers that histidine can bridge between copper and either zinc, cobalt, or a second copper atom. The suggestion of a histidine bridge between copper and iron would thus seem plausible.

When Cu<sub>B</sub> is oxidized, the sixth coordination site of cytochrome *a*<sub>3</sub> is left vacant, thus ensuring the high-spin state as established by our MCD data, but in order to achieve the known inertness of ferricytochrome *a*<sub>3</sub> with typical heme ligands, we propose a part of the polypeptide chains blocks access to the vacant coordination site. (The presence of a weak-field sixth ligand cannot be ruled out but this has no immediate bearing on our scheme.) Cu<sub>B</sub><sup>2+</sup> is assigned a reduction potential comparable to cytochrome *a*; cytochrome *a*<sub>3</sub> is assigned a more negative potential, closer to Cu<sub>A</sub><sup>2+</sup> (16).

A crucial piece of experimental data for testing the proposed structure(s) is the magnetic susceptibility of the enzyme; unfortunately, there are only a limited number of measurements in the literature (25–27). The more recent measurement shows

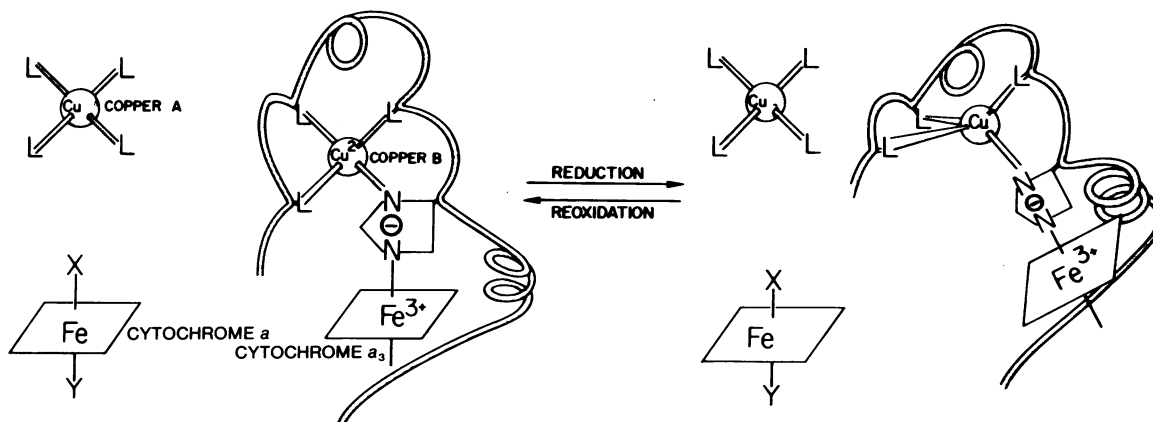


FIG. 2. Schematic representation of the composition of the active center of cytochrome oxidase as proposed in this paper. The changes that occur on the one electron reduction of the antiferromagnetically coupled Cu<sub>B</sub><sup>2+</sup> are also depicted. To avoid specifying the order of addition of electrons or the degree of reduction, the valence(s) of cytochrome *a* and Cu<sub>A</sub><sup>2+</sup> (EPR detectable) are omitted. The change in availability of the sixth coordination site of cytochrome *a*<sub>3</sub> is shown as a shift in the heme with respect to the polypeptide chain.

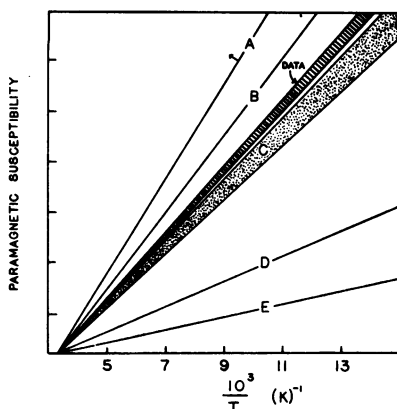


FIG. 3. Comparison of the magnetic susceptibility data of Tsudzuki and Okunuki (26) with several structural models. The experimental data delimit the cross-hatched zone, the upper margin shows results obtained with resting enzyme, and the lower margin the data recorded on native enzyme in the presence of excess sodium fluoride. The structural models considered are (A) single isolated low-spin heme plus isolated  $\text{Cu}^{2+}$  plus ferromagnetically coupled high-spin  $\text{Fe}^{3+}$  and  $\text{Cu}^{2+}$ , (B) magnetically isolated high- and low-spin hemes plus two isolated  $\text{Cu}^{2+}$ , (C) magnetically isolated low-spin heme plus isolated  $\text{Cu}^{2+}$  plus anti-ferromagnetically coupled high-spin  $\text{Fe}^{3+}$  and  $\text{Cu}^{2+}$ , (D) two isolated low-spin hemes plus two isolated  $\text{Cu}^{2+}$ , (E) single isolated low-spin heme plus an antiferromagnetically-coupled trimer (4) of a low-spin heme and two  $\text{Cu}^{2+}$ . The stippled zone represents the range of magnetic susceptibilities possible for alternative C assuming both spin and spin-plus-orbital contributions to  $\mu_{\text{eff}}^2$  ( $S = 2$ ).  $T$  = temperature.

the susceptibility to be linear from 77 K to 250 K (26) indicating that the postulated coupling between  $\text{Cu}_B^{2+}$  and cytochrome  $a_3$  must be quite strong with  $J$  (exchange coupling constant)  $\leq -200 \text{ cm}^{-1}$ . Also shown are the susceptibilities predicted for the model described here (Fig. 3, line C) together with a number of alternative possibilities. Of these, possibilities B and C fit the observed data most closely. Possibility B, however, assumes the existence of a magnetically normal high-spin heme EPR in the resting enzyme. Thus alternative C, the prediction of the model of Fig. 2, would seem to be the most plausible, accounting for more than 80% of the observed susceptibility.

In the early stages of a reductive titration, the species reduced at equilibrium will be cytochrome  $a$  and  $\text{Cu}_B^{2+}$ . This will result in (4), a loss of the EPR resonance at  $g = 3.05$  characteristic of

cytochrome  $a$  as it is reduced to the low-spin ferrocyclochrome  $a$  and (4) the conversion of  $\text{Cu}_B$  to the diamagnetic cuprous form. We propose that this occurs with a conformational change in the protein such that access to the sixth site of cytochrome oxidase is no longer blocked and heme ligands are now free to react with the ferric ion of cytochrome  $a_3$ . This change could be triggered by reduction of either cytochrome  $a$  or  $\text{Cu}_B^{2+}$  and with the presently available data it is not possible to resolve this point. For illustrative purposes only, we depict the conformational change as a consequence of a change in the coordination geometry at  $\text{Cu}_B^{2+}$  (Fig. 2); however, we stress that we do not favor this possibility over the alternative and, indeed, there are some data that are best explained by invoking heme  $a$  as the focus of the conformational change. The second consequence of reduction of the copper is that it is no longer paramagnetic, thus destroying the antiferromagnetic coupling between  $\text{Cu}_B$  and cytochrome  $a_3$ ; consequently the EPR of a high-spin heme ( $S = 5/2$ ) should appear. It is indeed observed experimentally that a high-spin  $\text{Fe}^{3+}$  EPR signal appears in partially reduced enzyme and addition of heme-ligands, e.g., azide, to such a partially reduced enzyme leads to a rapid disappearance of the high-spin EPR with a concomitant appearance of a low-spin EPR signal (5). Because the decrease in the magnetic susceptibility of  $\text{Cu}_B$  is smaller than the increment in susceptibility in going from  $S = 2$  to  $S = 5/2$ , the room temperature magnetic susceptibility of the enzyme should increase during this phase of the titration (Fig. 4, right).

Further addition of electrons should then lead to a disappearance of both the copper and the high-spin heme EPR signals, as  $\text{Cu}_A^{2+}$  is reduced to  $\text{Cu}_A^{1+}$  and the high-spin ferricytochrome  $a_3$  is converted to a high-spin ferrocyclochrome  $a_3$ , as implied by our MCD results. The magnetic susceptibility of the reduced enzyme will remain high.

On reoxidation these events should be reversed: the high-spin EPR signal of cytochrome  $a_3$  will appear as the iron atom is oxidized, subsequently disappearing as  $\text{Cu}_B$  is reoxidized re-establishing the antiferromagnetic interaction between the two centers  $\text{Cu}_B^{2+}$  and  $\text{Fe}_{a_3}^{3+}$ . This latter step is accompanied by a reversal of the conformational change (Fig. 2) which thus renders the high-spin iron atom once more inaccessible to added reagents.

Using the proposal of Fig. 2, we have simulated the recent EPR data of Hartzell and Beinert (28). In Fig. 4 (left) we fit the data for the four component titration of  $\text{Cu}_A^{2+}$ ,  $\text{Cu}_B^{2+}$ , cytochrome  $a$ , and cytochrome  $a_3$ . All of the features of the data are

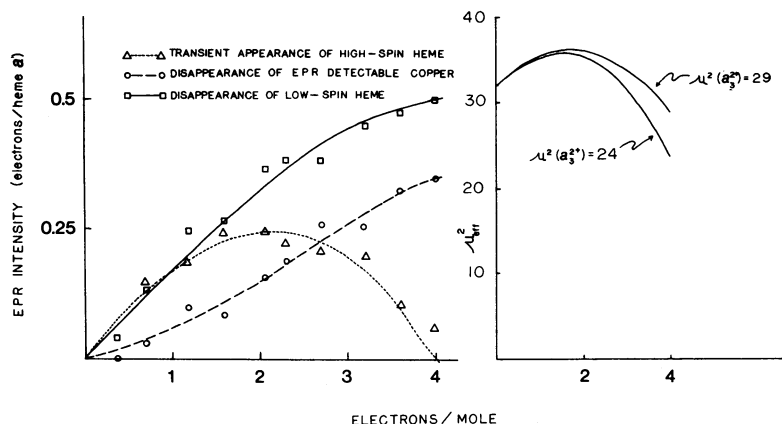


FIG. 4. Simulation of the EPR signals (left) and predicted variation in magnetic susceptibility (right) during a reductive titration. The calculations follow the procedures of ref. 34 with relative equilibrium constants of 1, 1.8, 0.1, and 0.6 for the reduction of cytochrome  $a^{3+}$ ,  $\text{Cu}_A^{2+}$ , cytochrome  $a_3^{3+}$ , and  $\text{Cu}_B^{2+}$ , and assume that the maximum changes are 0.5, 0.35, and 0.25 mol/mol total heme  $a$ , for cytochrome  $a$ ,  $\text{Cu}_B^{2+}$ , and total high spin-heme, respectively. The symbols represent the data of Hartzell and Beinert (28).

reproduced including the biphasic behavior of the high-spin heme; the appearance of the high-spin EPR in the early part of the titration is a consequence of the elimination of the antiferromagnetic coupling with  $a_3$  as  $\text{Cu}_B^{2+}$  is reduced to the diamagnetic cuprous state, with the subsequent reduction of  $a_3$  next during the later stages of the titration. The marked lag in the disappearance of  $\text{Cu}_A^{2+}$  signal is also reproduced. With these equilibrium constants, one can also calculate the magnetic susceptibility of cytochrome oxidase throughout a reductive titration (Fig. 4, right). As described above, the susceptibility increases initially by a small amount, being maximal at approximately 50% reduction, thereafter decreasing to a final high value typical of high-spin  $\text{Fe}^{2+}$ . A small increase in susceptibility on partial reduction has been reported previously (27).

This calculation yields only the relative potentials of the four species. To obtain the absolute potentials, a 5-component fit was made to the data of Hartzell and Beinert (28) from an experiment in which cytochrome *c* is also present. The values obtained are approximately 350, 340, 305, and 200 mV for  $\text{Cu}_B$ , cytochrome *a*,  $\text{Cu}_A$ , and cytochrome  $a_3$ , respectively. With the exception of  $\text{Cu}_A$ , which is reported to have a potential close to 230 mV (16), these values are in semiquantitative agreement with values obtained potentiometrically; the discrepancy seen in the potential for  $\text{Cu}_A$  is substantial, but inspection of Hartzell and Beinert's data show clearly that this species must be more oxidizing than cytochrome *c* under the conditions of the experiments. It seems plausible that with the high concentrations of oxidase and cytochrome *c* employed, the two proteins are present as a complex which has reduction potentials somewhat modified from those observed with the free oxidase.

The scheme of Fig. 2 provides a rational interpretation of the observation that addition of CO to a partially reduced sample of the oxidase reduces the high-spin EPR signal of  $a_3$  and increases the low-spin EPR signal of cytochrome *a* (16). As CO binds very avidly to reduced cytochrome  $a_3$ , and only poorly to oxidized cytochrome  $a_3$ , the reduction potential of the cytochrome  $a_3$ -CO complex will be much more positive than that of cytochrome *a* (16). Thus, addition of CO to partially-reduced oxidase makes cytochrome  $a_3$  the best oxidant, with the result that it becomes reduced at the expense of the other electron donors present in the enzyme. Consequently, the high-spin EPR diminishes as ferricytochrome  $a_3$  becomes reduced while the EPR of low-spin ferricytochrome *a* intensifies as its metal becomes oxidized. Photolysing off the carbon monoxide restores the original potential of cytochrome  $a_3$  and the electron distribution is then able to relax to its initial state which restores the original intensity of the EPR signals, and demonstrates that these intramolecular electron transfer processes proceed efficiently even at cryogenic temperatures.

In the presence of ATP, the potential of the  $a_3$ -CO compound varies with the concentration of CO, but the Nernst plot exhibits a  $n = 2$ , implying that the electron transfer process utilizes two electrons (29). One can easily show that the ordered addition of two electrons to the  $\text{Cu}_B^{2+}$ - $a_3$  pair leads to Nernst plots with slopes which vary continuously from 1 [when  $E'_0$  for  $a_3 < E'_0$  for  $\text{Cu}_B$  (no CO)] to 2 [when  $E'_0$  for  $a_3 > E'_0$  for  $\text{Cu}_B$  (saturating CO)]. An assumed value of 410 mV for  $E'_0$  ( $a_3$ ) under 1 atm ( $1 \times 10^5$  pascal) CO is equivalent to a dissociation constant for the binding of CO- $a_3^{3+}$  about 2400 times larger than that for  $a_3^{2+}$ , namely 1 mM compared with 0.4  $\mu\text{M}$ . However, because of the proposed conformational change there may be a kinetic barrier to the formation of  $a_3^{3+}$ -CO and its existence will be difficult to demonstrate except at high concentrations of ligand, and with long incubation times. Addition of potassium ferricyanide to the reduced oxidase-CO complex should lead to a rapid reox-

idation. However, as soon as  $\text{Cu}_B^{2+}$  and/or cytochrome *a* becomes reoxidized the original conformation is restored: the inability of ferricyanide to completely oxidize the CO complex (30) can now be interpreted as a consequence of steric hindrance resulting from the restoration of the original conformation.

The proposals of Fig. 2 also provide a rational explanation of the anomalous Mossbauer results of Lang *et al.* (31), who observed features in the Mossbauer spectrum of oxidized protein at 195 K consistent with the presence of a high-spin heme. These spectral features persist at lower temperatures whereas previous experience would require that they change over to a characteristic six-line pattern extending over a large spectral range (*ca* 10  $\text{mm s}^{-1}$ ), reflecting the large increase of the electron spin relaxation time for mononuclear high-spin ferric ion as the temperature is lowered. A spin-coupled dimer with  $S = 2$  is expected to have much more rapid electron spin relaxation and thus even at 4.2 K the average hyperfine field produced by the Fe electrons at the iron nucleus will be small and the wide magnetic hyperfine pattern expected for a slowly relaxing species will be replaced by the collapsed spectrum characteristic of the fast relaxation regime.

Hartzell *et al.* (32) have identified a weak absorption band at 655 nm which decreases in intensity during a reductive titration as the high-spin EPR signals appear; a corresponding derivative shaped curve is seen at 665 nm in the MCD spectrum (10). Accordingly, it would seem that this band arises from heme  $a_3$  as a consequence of the antiferromagnetic interaction. One possibility requires that the transition be an exchange-enhanced spin forbidden band of high-spin  $\text{Fe}^{3+}$ , for example, the  ${}^6A \rightarrow {}^4T$  ( $d-d$ ) transition: the observed extinction coefficient seems too large to make this alternative very persuasive. A second possibility is that the 655 nm band is porphyrin ( $\pi$ )  $\rightarrow$  metal ( $d$ ) charge transfer and that the decrease in intensity at 655 nm is due to the shifting of the band to shorter wavelengths, rather than a bleaching diagnostic of reduction: thus, reduction of  $\text{Cu}_B^{2+}$  to the cuprous form releases charge to the bridging histidine which then becomes a stronger ligand to the iron with a consequent increase in the energy of this transition (33).

When reduced cytochrome oxidase is oxygenated under a variety of conditions, the product has a Soret maximum at 428 nm (ref. 34 and references therein). This species then slowly changes to one with a Soret maximum at *ca* 419 nm, typical of the resting oxidized enzyme. Tiesjma *et al.* (34) have shown that the oxygenated oxidase only requires 4 reducing equivalents for full reduction: it thus seems improbable that additional oxidizing equivalents are trapped in the oxygenated form. One can envision that under certain conditions one of the reduced products of  $\text{O}_2$  is unable to dissociate from the  $a_3$  before the oxidized conformation is reestablished. As the MCD of the oxygenated oxidase (10) is very similar to that of the oxidized enzyme shown in Fig. 1, no additional low-spin species is created and it seems probable that  $\text{H}_2\text{O}$  is the trapped ligand which, with time, dissociates and restores the true oxidized form of the enzyme. Support for this notion comes from the observation (35) that an Fe-azide infrared stretch can only be demonstrated *after* oxidase has been reoxidized in the presence of sodium azide; prolonged incubation of the ferric oxidase with azide is unable to produce any metal-ligand infrared bands.

The proposed antiferromagnetic coupling between cytochrome  $a_3$  and  $\text{Cu}^{2+}$  provides an attractive explanation for a number of salient observations on the properties of cytochrome oxidase. This enzyme is, however, much more complex than might be inferred from the preceding discussion. Thus, it is attractive to speculate that the twin devices of establishing

cytochrome  $a_3$  as the least oxidizing component, and the conformational change subsequent to reduction, exist to ensure that reduced oxidase will normally not react with oxygen until the enzyme is fully reduced, and will thus avoid pathological side reactions.

The proposal of structures such as those embodied in Fig. 2 are a necessary first step for any quantitative characterization of this enzyme and, as a very minimum, suggest a variety of feasible experiments which can be used to probe the validity of such structures. In so doing, the proposals provide additional valuable insight into the properties of this enzyme.

We are indebted to Dr. Helmut Beinert for graciously allowing us the use of his data prior to publication and for provocative discussion of some of the ideas presented, and to Dr. Winslow Caughey for a copy of his review in advance of publication. This work was supported by grants from the National Institutes of Health (GM 121703), the Welch Foundation and ERDA, and by a postdoctoral fellowship (G.T.B.) from the National Institutes of Health (HL 02052).

1. Mackey, L. N., Kuwana, T. & Hartzell, C. R. (1973) *FEBS Lett.* **36**, 326–329.
2. Chance, B., Saronio, C. & Leigh, J. S. (1975) *J. Biol. Chem.* **250**, 9226–9237.
3. Beinert, H., Griffiths, D. E., Wharton, D. C. & Sands, R. H. (1962) *J. Biol. Chem.* **237**, 2337–2346.
4. Malmstrom, B. G. (1973) *Q. Rev. Biophys.* **6**, 389–431.
5. Van Gelder, B. F. & Beinert, H. (1969) *Biochim. Biophys. Acta* **189**, 1–24.
6. Beinert, H., Hansen, R. E. & Hartzell, C. R. (1976) *Biochim. Biophys. Acta* **423**, 339–355.
7. Wever, R., Muijers, A. O., Van Gelder, B. F., Bakker, E. P. & Van Buren, K. J. H. (1973) *Biochim. Biophys. Acta* **325**, 1–7.
8. Antonini, E., Brunori, M., Greenwood, C., Malmstrom, B. G. & Rotilio, G. C. (1971) *Eur. J. Biochem.* **23**, 396–400.
9. Wever, R., Van Gelder, B. F. & Dervartanian, D. V. (1975) *Biochim. Biophys. Acta* **387**, 189–193.
10. Babcock, G. T., Vickery, L. & Palmer, G. (1976) *Biophys. J.* **16**, 87a.
11. Vickery, L., Nozawa, T. & Sauer, K. (1976) *J. Am. Chem. Soc.* **98**, in press.
12. Treu, J. I. & Hopfield, J. J. (1975) *J. Chem. Phys.* **63**, 613–623.
13. Sutherland, J. C., Vickery, L. E. & Klein, M. P. (1974) *Rev. Sci. Instrum.* **45**, 1089–1094.
14. Palmer, G. (1976) in *The Porphyrins*, ed. Dolphin, D. (Academic Press, New York), in press.
15. Griffith, J. S. (1971) *Mol. Phys.* **21**, 141–143.
16. Leigh, J. S., Wilson, D. F., Owen, C. S. & King, T. P. (1974) *Arch. Biochem. Biophys.* **160**, 476–486.
17. Sugiura, Y., Hirayama, Y. & Tanaka, H. J. (1975) *Am. Chem. Soc.* **97**, 5577–5581.
18. Brill, A. & Bryce, G. (1968) *J. Chem. Phys.* **48**, 4398–4409.
19. Blokzijl-Homan, M. F. & Van Gelder, B. F. (1971) *Biochim. Biophys. Acta* **234**, 493–498.
20. Gibson, Q. H. & Greenwood, C. (1963) *Biochem. J.* **86**, 541–553.
21. Yonetani, T. Y. & Yamamoto, H. (1973) in *Oxidases and Related Enzyme Systems*, eds. King, T. E., Mason, H. S. & Morrison, M. (University Park Press, Baltimore, Md.), pp. 279–299.
22. Richardson, J. S., Thomas, K. A., Rubin, B. H. & Richardson, D. C. (1975) *Proc. Natl. Acad. Sci. USA* **72**, 1349–1353.
23. Fee, J. A. & Briggs, A. G. (1975) *Biochim. Biophys. Acta* **400**, 439–450.
24. Moss, T. H. & Fee, J. A. (1975) *Biochem. Biophys. Res. Commun.* **66**, 799–808.
25. Ehrenberg, A. & Yonetani, T. Y. (1961) *Acta Chem. Scand.* **15**, 1071–1080.
26. Tsudzuki, T. & Okunuki, K. (1971) *J. Biochem.* **69**, 909–922.
27. Ehrenberg, A. & Vanneste, W. (1968) *19th Colloquium der Gesellschaft fuer Biologische Chemie, Mosbach*, (Springer, New York), pp. 121–124.
28. Hartzell, C. R. & Beinert, H. (1976) *Biochim. Biophys. Acta* **423**, 323–338.
29. Lindsey, J. S. & Wilson, D. F. (1974) *FEBS Lett.* **48**, 45–49.
30. Wharton, D. C. (1964) *Biochim. Biophys. Acta* **92**, 607–609.
31. Lang, G., Lippard, S. J. & Rosen, S. (1974) *Biochim. Biophys. Acta* **336**, 6–14.
32. Hartzell, C. R., Hansen, R. E. & Beinert, H. (1973) *Proc. Natl. Acad. Sci. USA* **70**, 2477–2481.
33. Morell, D. B., Barrett, J., Clezy, P. & Lemberg, R. (1961) in *Hematin Enzymes*, eds. Falk, V. E., Lemberg, R. & Morton, R. K. (Pergamon Press, Oxford, England), pp. 320–335.
34. Tiejma, R. H., Muijers, A. O. & Van Gelder, B. F. (1972) *Biochim. Biophys. Acta* **256**, 32–42.
35. Caughey, W. S., Wallace, W. J., Volpe, J. A. & Yoshikawa, S. (1976) in *The Enzymes*, ed. Boyer, P. D. (Academic Press, New York), Vol. 13, in press.